Homoclinic bifurcation sets of the parametrically driven Duffing oscillator

S. Parthasarathy
Centre for Nonlinear Dynamics, Department of Physics, Bharathidasan University, Tiruchirapalli 620 024, India
(Received 21 December 1990)

Using the Melnikov-function approach, we obtain the threshold condition for the occurrence of Smale-horseshoe chaos in the parametrically driven Duffing oscillator. A detailed description of the homoclinic bifurcation sets in the five-dimensional parameter space involved in the system is provided.

PACS number(s): 05.45.+b, 47.20.Tg, 47.20.Ky, 89.90.+n

We consider the Duffing oscillator [1] subjected to (i) an external periodic force with amplitude F_1 having circular frequency ω_1, and (ii) a parametrically driven force having amplitude F_2 with circular frequency ω_2. The resultant equation of motion of the parametrically driven Duffing oscillator, restricted to the case for which the external and parametric forcings are in phase, is given by

$$\ddot{x}+\epsilon\alpha\dot{x}-(1+\epsilon F_2\cos\omega_2 t)x+x^3=\epsilon F_1\cos\omega_1 t \;, \quad (1)$$

where α denotes viscous damping and ϵ ($\ll 1$) is a perturbation parameter and an overdot means differentiation with respect to t. Apart from various applications of the Duffing oscillator [$F_2=0$ in Eq. (1)] which system (1) can have, it also serves as a model for the driven Rayleigh-Bénard convection [2–5] and nonlinear electrical networks and mechanical systems [6].

For $F_2=0$, Eq. (1) represents the forced Duffing oscillator for which the threshold for the occurrence of Smale-horseshoe chaos was already studied [7] in detail. Apart from a single force, the effect of a number of competing external forcing frequencies on the region of chaos in the quasiperiodically forced Duffing oscillator has also been investigated [8–10] recently. With $F_1=0$, Eq. (1) gives the parametrically driven Duffing oscillator, which has a form similar to the nonlinear Mathieu equation [11]. We consider here the combined effect of both the external force and the parametrically driven force in the Duffing oscillator, along with viscous damping on the threshold for the occurrence of Smale-horseshoe chaos in the system.

Considering Eq. (1), when $\epsilon=0$, the system is obviously integrable and possesses a separatrix orbit [12], which is a basic requirement for the application of the Melnikov method [12,13]. In this paper we wish to obtain the criterion for the occurrence of Smale-horseshoe chaos in system (1) when $\epsilon\neq 0$, and investigate the effect of both the external forcing and parametric excitation on the homoclinic bifurcation set in the five-dimensional parameter space $(\alpha,F_1,F_2,\omega_1,\omega_2)$ obtained from the Melnikov function. Our study goes much beyond the earlier work of Newton [5] and gives a complete classification of the bifurcation sets in the parameter space of Eq. (1) along the lines of Ide and Wiggins [10]. From these results we can predict for a given set of parameters whether transverse intersections of the stable and unstable manifolds of the corresponding Poincaré map occur in the parametrically driven Duffing oscillator (1), and can also obtain the threshold for the occurrence of Smale-horseshoe chaos in the system.

The Melnikov method [12,13] is perhaps the only analytical tool currently available to provide a criterion for the occurrence of Smale-horseshoe chaos in a system. Since this method has been described many times by different authors [7–10,12–14], we do not discuss it in detail here, but present only the results. We begin by rewriting Eq. (1) as two coupled first-order ordinary differential equations:

$$\dot{x}=y \;, \qquad \dot{y}=x-x^3+\epsilon(F_1\cos\omega_1 t+F_2 x\cos\omega_2 t-\alpha y) \;. \quad (2)$$

The unperturbed system has three fixed points: a hyperbolic fixed point at (0,0) and two elliptic fixed points at $(\pm 1,0)$. It also possesses a separatrix solution

$$(x_0,y_0)=(\sqrt{2}\,\mathrm{sech}\,\tau,\ -\sqrt{2}\,\mathrm{sech}\,\tau\tanh\tau) \;, \quad \tau=t-t_0 \quad (3)$$

known as the separatrix orbit, passing through the hyperbolic fixed point. In order to determine a criterion for the occurrence of transverse intersections of the stable and unstable manifolds of the corresponding Poincaré map, we compute the Melnikov function, which in this case takes the form

$$M(t_0)=\int_{-\infty}^{\infty} y_0(\tau)[F_1\cos\omega_1(\tau+t_0)+F_2\cos\omega_2(\tau+t_0)x_0(\tau)-\alpha y_0(\tau)]d\tau \;. \quad (4)$$

Using Eq. (3) in Eq. (4) and evaluating the resulting integrals, we get

$$M(t_0)=\sqrt{2}\,F_1\pi\omega_1\mathrm{sech}(\pi\omega_1/2)\sin\omega_1 t_0+F_2\pi\omega_2^2\mathrm{cosech}(\pi\omega_2/2)\sin\omega_2 t_0-4\alpha/3 \;. \quad (5)$$

From Eq. (5) one can easily write the criterion for the occurrence of Smale-horseshoe chaos as

$$\alpha\le\alpha_c=\tfrac{3}{4}f_1\omega_1\mathrm{sech}(\pi\omega_1/2)+\tfrac{3}{4}f_2\omega_2^2\mathrm{cosech}(\pi\omega_2/2) \;, \quad (6)$$

where $f_1=\sqrt{2}\,\pi F_1$ and $f_2=\pi F_2$. Thus for a given value of $f_1,f_2,\omega_1,\omega_2$ we can find the critical value of the damping α_c using Eq. (6) and predict that, for any $\alpha<\alpha_c$ transverse intersections of the stable and unstable manifolds of the corresponding Poincaré map occur and the system exhibits chaotic behavior or transient chaos [15] followed by periodic motion.

Using Eq. (6) we can obtain the homoclinic bifurcation sets of the parametrically driven Duffing oscillator. In the five-dimensional parameter (i.e., $\alpha,f_1,f_2,\omega_1,\omega_2$) space the bifurcation set is given by the four-dimensional surface represented mathematically by Eq. (6). One useful way of representing this surface is to use the method recently adopted by Ide and Wiggins [10] in connection with the two competing quasiperiodic external forces and to present bifurcation curves in the ω_1-ω_2 plane for fixed values of α,f_1,f_2. We divide the (α,f_1,f_2) space into 20 different sections, as considered by Ide and Wiggins [10], which enables us to cover the entire (α,f_1,f_2) space and obtain the bifurcation curves in the ω_1-ω_2 plane.

Now let us see how to obtain the bifurcation curve in the ω_1-ω_2 plane for a chosen set of values of (α,f_1,f_2). Defining

$$X_1=\omega_1 \mathrm{sech}(\pi\omega_1/2)\ ,\quad X_2=\omega_2^2 \mathrm{cosech}(\pi\omega_2/2)\ , \tag{7a}$$

Eq. (6) can be rewritten as

$$-\tfrac{4}{3}\alpha+f_1X_1+f_2X_2=0\ . \tag{7b}$$

Equation (7b) is linear in f_1,f_2,X_1, and X_2 and can be regarded as a hyperplane in the (α,f_1,f_2,X_1,X_2) space. It degenerates into a straight line in the X_1-X_2 plane for fixed α,f_1,f_2. Then using the form of (X_1,X_2) in terms of (ω_1,ω_2), as given by Eq. (7a), we can map the bifurcation curves in the X_1-X_2 plane back into bifurcation curves in the ω_1-ω_2 plane.

The nature of X_1 and X_2 and their inverses can be inferred from Figs. 1(a) and 1(b). Figure 1(a) shows that the functions X_1 and X_2 (i) have their maximum values at ω_1' and ω_2', (ii) are strictly increasing for $0<\omega_1<\omega_1'$ and $0<\omega_2<\omega_2'$, and (iii) are decreasing for $\omega_1>\omega_1'$ and $\omega_2>\omega_2'$, respectively. Figure 1(b) depicts the inverse functions $\omega_1(X_1)$ and $\omega_2(X_2)$. These are doubled-valued functions and their increasing and decreasing branches are denoted ω_1^+,ω_2^+ and ω_1^-,ω_2^-, respectively.

In order to obtain the bifurcation lines in the X_1-X_2 plane, we rewrite Eq. (7) as

$$X_2=\frac{1}{f_2}(-f_1X_1+\tfrac{4}{3}\alpha)\ ,\quad 0\le X_1\le X_1'\ ,\quad 0\le X_2\le X_2' \tag{8}$$

and solve for the value of X_2 for the values of X_1 equal to 0 and X_1'. For example, when $\alpha=\frac{3}{4}f_2X_2'$ and $0<f_1<f_2$ one can easily find from Eq. (8) that $X_2=X_2'$ for $X_1=0$ while $X_2<X_2'$ for $X_1=X_1'$. By connecting these two points, we obtain the corresponding bifurcation line in the X_1-X_2 plane as shown in Fig. 2(a). It is evident [cf. Eq. (6)] that transverse homoclinic orbits occur only in the hatched region of Fig. 2(a). This bifurcation line in the X_1-X_2 plane can be converted into a bifurcation curve in the ω_1-ω_2 plane. From Fig. 1(b), we note that for each value of (X_1,X_2) in the hatched region of Fig. 2(a), there are two values of (ω_1,ω_2). Using this fact, along with the shapes of $\omega_1(X_1)$ and $\omega_2(X_2)$, shown in Fig. 1(b), we map the bifurcation line in the X_1-X_2 plane back into the bifurcation curve in the ω_1-ω_2 plane, inside which transverse homoclinic orbits occur. This is shown in Fig. 2(b).

Using the above procedure, the bifurcation set in the ω_1-ω_2 plane can be obtained for all 20 different sections of (α,f_1,f_2) space. Figure 3 displays the complete homoclinic bifurcation sets in the ω_1-ω_2 plane, along with the corresponding bifurcation sets in the X X_2 plane for the 20 different sections of (α,f_1,f_2) space. We have also provided the values of α,f_1, and f_2 for all 20 different sections of (α,f_1,f_2) space considered here in the legend of Fig. 3.

From Fig. 3 (cases 1–20) we can observe the following interesting possibilities of homoclinic bifurcation sets for

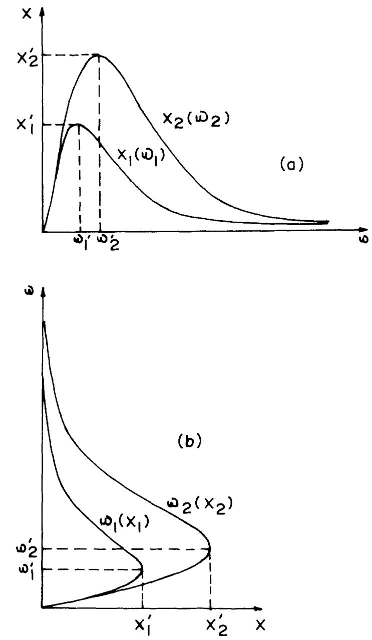

FIG. 1. (a) Graph of $X_1(\omega_1)$ and $X_2(\omega_2)$ and (b) graph of $\omega_1(X_1)$ and $\omega_2(X_2)$.

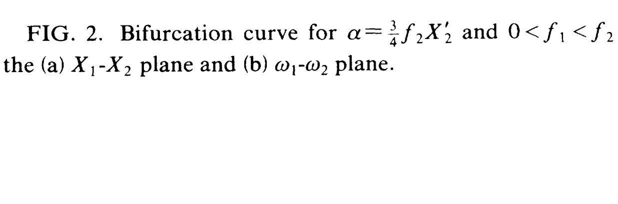

FIG. 2. Bifurcation curve for $\alpha=\frac{3}{4}f_2X_2'$ and $0<f_1<f_2$ in the (a) X_1-X_2 plane and (b) ω_1-ω_2 plane.

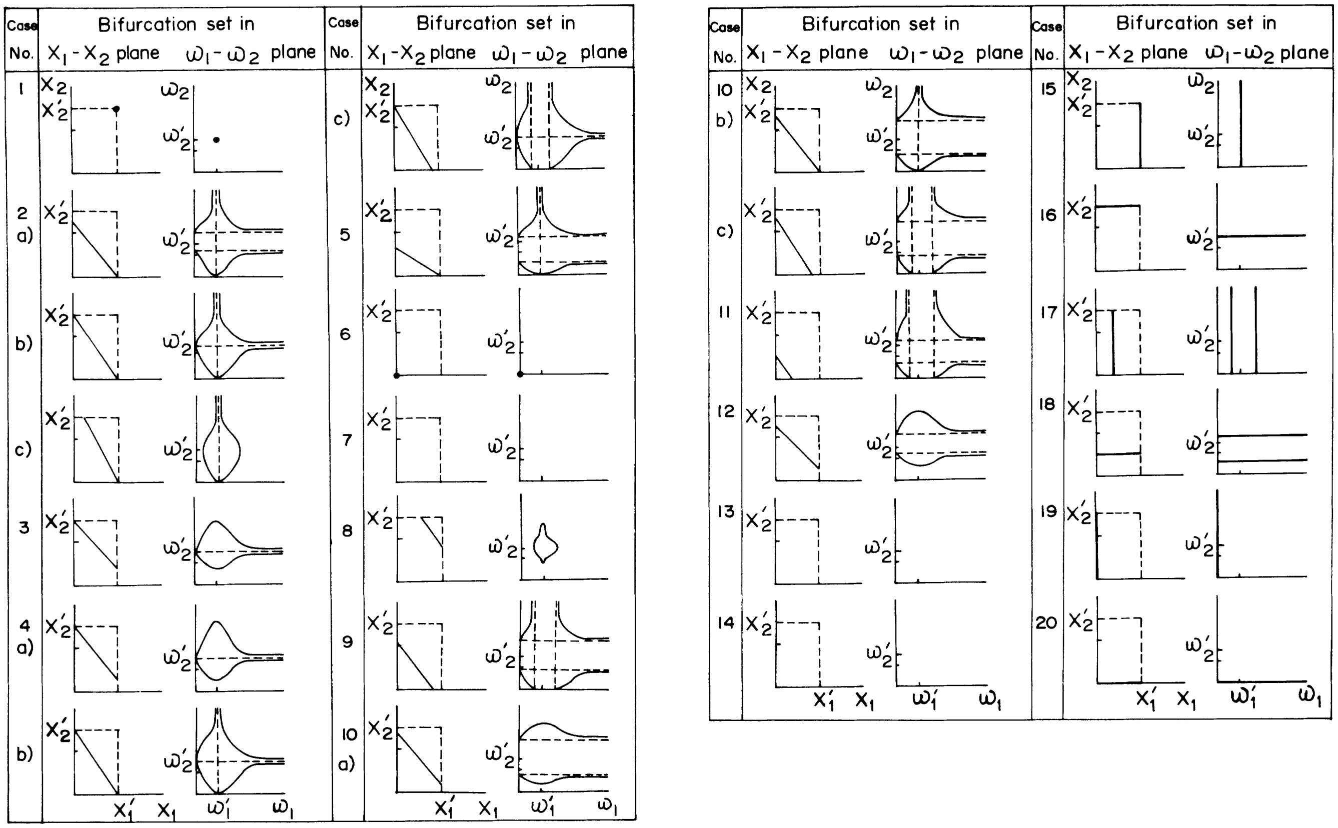

FIG. 3. The complete homoclinic bifurcation sets of the parametrically driven Duffing oscillator in the X_1-X_2 plane and ω_1-ω_2 plane for the 20 different sections of (α,f_1,f_2) space, viz., (1) $\alpha=\frac{3}{4}(f_1X_1'+f_2X_2')$, $f_1>0,f_2>0$; (2) $\alpha=\frac{3}{4}f_1X_1'$, $f_1>f_2>0$, (a) $X_1'<X_2<X_2'$, (b) $X_2=X_2'$, (c) $X_2>X_2'$; (3) $\alpha=\frac{3}{4}f_2X_2'$, $0<f_1<f_2$; (4) $\alpha=\frac{3}{4}f_2X_2'$, $f_1>f_2>0$, (a) $0<X_2<X_1'$, (b) $X_2=0$, (c) $X_2<0$; (5) $\alpha=\frac{3}{4}f_1X_1'$, $0<f_1<f_2$; (6) $\alpha=0$, $f_1>0$, $f_2>0$; (7) $\alpha>\frac{3}{4}(f_1X_1'+f_2X_2')$, $f_1>0$, $f_2>0$; (8) $\frac{3}{4}(f_1X_1'+f_2X_2')>\alpha>\frac{3}{4}\sup\{f_1X_1',f_2X_2'\}$, $f_1>0$, $f_2>0$; (9) $\frac{3}{4}f_1X_1'>\alpha>\frac{3}{4}f_2X_2'$, $f_1>f_2>0$; (10) $\frac{3}{4}f_2X_2'>\alpha>\frac{3}{4}f_1X_1'$, $0<f_1<f_2$, (a) $0<X_2<X_1'$, (b) $X_2=0$, (c) $X_2<0$; (11) $0<\alpha<\frac{3}{4}\inf\{f_1X_1',f_2X_2'\}$, $f_1>0$, $f_2>0$; (12) $\alpha=\frac{3}{4}[(f_1X_1'+f_2X_2')/2]$, $f_1=f_2>0$; (13) $\alpha>\frac{3}{4}f_1X_1'$, $f_1>0$, $f_2=0$; (14) $\alpha>\frac{3}{4}f_2X_2'$, $f_1=0$, $f_2>0$; (15) $\alpha=\frac{3}{4}f_1X_1'$, $f_1>0$, $f_2=0$; (16) $\alpha=\frac{3}{4}f_2X_2'$, $f_1=0$, $f_2>0$; (17) $0<\alpha<\frac{3}{4}f_1X_1'$, $f_1>0$, $f_2=0$; (18) $0<\alpha<\frac{3}{4}f_2X_2'$, $f_1=0$, $f_2>0$; (19) $\alpha=0, f_1>0, f_2=0$; (20) $\alpha=0, f_1=0, f_2>0$.

the parametrically driven Duffing oscillator.

(i) For the choice of $\alpha=\frac{3}{4}(f_1X_1'+f_2X_2')$, $f_1>0$, and $f_2>0$, homoclinic bifurcation occurs at exactly one point in the (ω_1,ω_2) plane given by $(\omega_1,\omega_2)=(\omega_1',\omega_2')$ (see case 1 in the figure).

(ii) For the choice of $\alpha=0$, $f_1>0$, and $f_2>0$, transverse homoclinic orbits exist for all values of ω_1 and ω_2 except for $\omega_1=\omega_2=0$ (see case 6).

(iii) For some choices of (α,f_1,f_2), there are no values of ω_1 and ω_2 for which homoclinic bifurcation occur (see cases 7, 13, and 14).

(iv) For many choices of (α,f_2,f_2), transverse homoclinic orbits exist only for the set of values of (ω_1,ω_2) which lie within the area enclosed by the bifurcation curves (see cases 2–5 and 8–12).

(v) For some other choices of (α,f_1,f_2), transverse homoclinic orbits exist only for the set of values of (ω_1,ω_2) which lie within the area enclosed by the bifurcation lines (see cases 17 and 18).

(vi) For other choices of (α,f_1,f_2), homoclinic bifurcation occurs at those values of (ω_1,ω_2) which lie on the bifurcation line (see cases 15, 16, 19, and 20).

Finally, upon comparing the nature of the bifurcation curves in the case of two competing external frequencies as studied by Ide and Wiggins [10], one notes that the form of $X_1(\omega_1)$ and $X_2(\omega_2)$ are similar where as in our case they are different [cf. Eq. (7a)] and possess different maximum values of X_1 and X_2 at ω_1 and ω_2, respectively. Correspondingly, the resulting bifurcation sets for system (1) also vary compared to those obtained by Ide and Wiggins [10] for the quasiperiodically forced Duffing oscillator, leading to different bifurcation sets in the ω_1-ω_2 plane for certain cases and to additional subcases in cases 2, 4, and 10.

The author expresses his sincere gratitude to Professor M. Lakshmanan for his constant guidance and continuous encouragement. This work forms part of a research project sponsored by the Council of Scientific and Industrial Research, India.

[1] G. Duffing, *Erzwugene Schwingungen bei veränderlicher Eigenfrequenz und ihre technische Bedetung* (Vieweg, Braunschweig, 1918).
[2] G. Ahlers, P. C. Hohenberg, and M. Lucke, Phys. Rev. Lett. **53**, 48 (1984).
[3] G. Ahlers, P. C. Hohenberg, and M. Lucke, Phys. Rev. A **32**, 3493 (1985); **32**, 3519 (1985).
[4] M. Lucke and F. Schauk, Phys. Rev. Lett. **54**, 1465 (1985).
[5] P. K. Newton, Phys. Rev. A **37**, 932 (1988).
[6] A. H. Nayfeh and D. T. Mook, *Nonlinear Oscillations* (Wiley-Interscience, New York, 1979).
[7] P. Holmes, Philos. Trans. R. Soc. London, Ser. A **292**, 419 (1979).
[8] S. Wiggins, Phys. Lett. A **124**, 138 (1987).
[9] S. Wiggins, *Global Bifurcations and Chaos—Analytical Methods* (Springer, New York, 1988).
[10] K. Ide and S. Wiggins, Physica D **34**, 169 (1989).
[11] T. T. Bowman, Nonlin. Anal. Theory, Methods Appl. **5**, 655 (1981).
[12] J. Gukenheimer and P. Holmes, *Nonlinear Osicllations, Dynamical Systems, and Vector Fields* (Springer, New York, 1983).
[13] V. K. Melnikov, Trans. Moscow Math. Soc. **12**, 1 (1963).
[14] S. Rajasekar, S. Parthasarathy and M. Lakshmanan, Chaos, Solitons Fractals (to be published).
[15] J. M. T. Thomson and H. B. Stewart, *Nonlinear Dynamics and Chaos* (Wiley, New York, 1986).